Ab Initio Calculation of Dynamic Polarizability and Dielectric Constant of Carbon and Silicon Cubic Crystals

DAVID AYMA,[1] JEAN PIERRE CAMPILLO,[1] MICHEL RÉRAT,[1] MAURO CAUSÀ[2]

[1]*Laboratoire de chimie structurale, UMR 5624, Université de Pau, IFR, rue J-Ferry, 64000 Pau, France*

[2]*Department of Inorganic, Physical and Materials Chemistry, University of Torino, Torino, Italy*

Received 11 March 1996; accepted 19 January 1997

ABSTRACT: Valence and conduction bands of carbon silicon cubic systems are first obtained by a process called linear combination of atomic orbitals self-consistent field (LCAO-SCF), both at the Hartree-Fock (HF) and local density approximation (LDA) levels. Then, the crystalline orbitals are used in a sum-over-states (SOS) method to calculate the corresponding dielectric constants related to electronic polarizabilities. This method allows parallel computations with large granularity of the optical properties and leads to uncoupled HF and LDA results. © 1997 by John Wiley & Sons, Inc. *J Comput Chem* **18**: 1253–1263, 1997

Keywords: *ab initio* LCAO-SCF calculation; Hartree-Fock (HF) and local density approximation (LDA) methods; frequency-dependent dielectric constant; parallel computation; diamond and silicon semiconductors

Introduction

The linear combination of atomic orbitals (LCAO) Hartree–Fock (HF) method, implemented in the CRYSTAL program[1] for periodic systems, generally leads to good descriptions of electronic density and thus to accurate properties, depending only on the valence band like elastic properties[2] and structure factors.[3]

Recently, Compton profiles, for which electronic correlation effects cannot be neglected,[4] have been also calculated using wave functions built from the density functional theory (DFT) in the local density approximation (LDA) included in CRYSTAL, by Causá and Zupan.[5]

In this work, whole sets of crystalline orbitals obtained by the CRYSTAL program at the HF and

Correspondence to: M. Rérat

Contract/grant sponsor: Human Capital and Mobility Program of the European Union; contract/grant number: CHRX-CT91-0155

Contract/grant sponsor: Centre National Universitaire Sud de Calcul

CCC 0192-8651 / 97 / 101253-11

LDA levels are stocked for regularly spaced $\vec{k}$-points of the reciprocal space. Then, in the second program where the approximate SOS method[6] allowing a parallel computation is implemented, we evaluate momentum matrix elements between each pair of previously occupied valence and empty conduction bands, in order to obtain static dielectric constant values and also frequency-dependent ones. This method which is very similar to the first principles of orthogonalized linear combination of atomic orbitals (OLCAO) studied and used by Ching et al.[7] (and references therein), is briefly presented in the first section. In the next section, parallel computational details are given, and in the last section the static values obtained in this work are compared with other results quoted in Refs. 8 and 9 or calculated in Ref. 10 for the two well-known C and Si covalent systems. Optical properties and energy loss functions of C and Si are also deduced from the variations of dynamic polarizabilities versus electric field frequency.

Method

UNPERTURBED WAVE FUNCTIONS

The crystalline orbitals of finite periodic systems are linear combinations of Bloch functions and are calculated by an SCF process with HF equations or by density functional theory (DFT) in local density approximation (LDA), where HF equations are replaced by Kohn–Sham (KS) equations. In both cases (HF/KS), the crystalline orbitals, $\Phi_l^{\vec{k}}(\vec{r})$, are solutions of the one-particle equation:

$$\hat{H}_0 \Phi_l^{\vec{k}}(\vec{r}) = \varepsilon_l^{\vec{k}} \Phi_l^{\vec{k}}(\vec{r})$$

where the monoelectronic $\hat{H}_0$ operator for regularly spaced $\vec{k}$-points is:

$$\hat{H}_0 = \hat{T} + \hat{V} + \hat{J} + \hat{K} \text{ in the HF case}$$

or

$$\hat{H}_0 = \hat{T} + \hat{V} + \hat{J} + \hat{\nu}^{x-c} \text{ in the KS scheme}$$

In both cases, $\hat{T}$, $\hat{V}$, and $\hat{J}$ are the kinetic, the external potential, and Coulomb operators, respectively. The exchange operator $\hat{K}$ of the HF method is replaced with the exchange-correlation potential $\hat{\nu}^{x-c}$ in the KS method. In fact, in the HF Hamiltonian, the exchange part is calculated exactly but the correlation is omitted, whereas in the KS method, the exchange and correlation parts are treated by different approximations. In this work, the Perdew–Zunger[11] parameterization of the numerical result, obtained by Ceperley–Alder,[12] for the electron gas, is chosen (for more details see Ref. 5).

POLARIZABILITY COMPONENTS

In the electric dipole Hamiltonian gauge, the expression of the polarizability components of a ground state is given by the following infinite sum:

$$\alpha_{uv} = 2 \sum_n^{\infty} \frac{\langle 0|u|n\rangle\langle n|v|0\rangle}{E_n - E_0} \quad u, v = x, y, \text{or } z$$

where $|0\rangle$ and $|n\rangle$ are, respectively, kets of the ground and excited states associated with the corresponding E_0 and E_n energies.

In our work, where $|0\rangle$ and $|n\rangle$ are described as products of monoelectronic $\phi_l^{\vec{k}}(\vec{r})$ functions for each $\vec{k}$-point, $\langle 0|u|n\rangle$ integrals are equal to $\langle \Phi_i^{\vec{k}}|u|\Phi_j^{\vec{k}}\rangle$ vertical transitions where i and j denote occupied and unoccupied crystalline orbitals, respectively, with the operator of perturbation $u(= x, y, \text{or } z)$ being monoelectronic (see Appendix for details concerning the calculation of these dipole moment integrals). This supposes that $|n\rangle$ are monoexcitations $|\Phi_i^{\vec{k}} \rightarrow \Phi_j^{\vec{k}}\rangle$ and the expression of α_{uv} becomes:

$$\alpha_{uv} = 2 \sum_{\vec{k}} \Omega(\vec{k}) \sum_{i,j} \frac{\langle \Phi_i^{\vec{k}}|u|\Phi_j^{\vec{k}}\rangle\langle \Phi_j^{\vec{k}}|v|\Phi_i^{\vec{k}}\rangle}{\varepsilon_j^{\vec{k}} - \varepsilon_i^{\vec{k}}} \quad (1)$$

where $\Omega(\vec{k})$ are geometrical weights associated with $\vec{k}$-points. In this expression, we consider that transition energies $E_n - E_0$ are equal to the differences between eigenvalues of $\Phi_i^{\vec{k}}$ and $\Phi_j^{\vec{k}}$; that is, dropping Coulomb $J_{ij}^{\vec{k}}$ and exchange $K_{ij}^{\vec{k}}$ terms which can be neglected if we consider that the interacting electron densities are completely diluted all over the crystal. The method is also an uncoupled perturbation method (UCHF or "UC LDA" according to $\hat{H}_0$ choice), because we do not take into account interactions between kets: $|n\rangle = |\Phi_i^{\vec{k}} \rightarrow \Phi_j^{\vec{k}}\rangle$ by the unperturbed Hamiltonian (even for the same $\vec{k}$-points) and then is less accurate than the random phase approximation (RPA) method extended to infinite systems [6] or the coupled Hartree–Fock (CHF) method with the velocity formula[10]. However, this method using unrelaxed orbitals can be easily extended to the time-dependent electric field. In this case we can

effectively assume that:

$$\alpha_{uv}(\omega) = \sum_{\vec{k}} \Omega(\hat{k}) \sum_{i,j} 2\left(\varepsilon_j^{\vec{k}} - \epsilon_i^{\vec{k}}\right) \times \frac{\langle \Phi_i^{\vec{k}} | u | \Phi_j^{\vec{k}} \rangle \langle \Phi_j^{\vec{k}} | v | \Phi_i^{\vec{k}} \rangle}{\left(\epsilon_j^{\vec{k}} - \epsilon_{\vec{k}}\right)^2 - \omega^2} \quad (2)$$

with ω being the electric field pulsation.

For nonionic systems, like diamond and silicon, the frequency-dependent dielectric constant is related to the dynamic atomic polarizability (or electric susceptibility) by the relation:

$$\frac{\varepsilon(\omega) - 1}{\varepsilon(\omega) + 2} = \frac{4\pi N}{3}\alpha(\omega)$$

with N being the number of atoms per unit volume.[8, 13, 14] In fact, the linear response $\alpha(\omega)$ function is a complex function from which the real part is calculated according to eq. (2) in the work. The imaginary part is related to the real one via Kramers–Kronig relation[8, 13, 14] so the mean $\alpha(\omega)$ polarizability is:

$$\alpha(\omega) = \sum_n f_n \left[\frac{\Delta E_n^2 - \omega^2}{(\Delta E_n^2 - \omega^2)^2 + \omega^2 \Gamma_n^2} + \frac{i\Gamma_n \omega}{(\Delta E_n^2 - \omega^2)^2 + \omega^2 \Gamma_n^2} \right] \quad (3)$$

where f_n and ΔE_n are oscillator strengths and transition energies, respectively, and $1/\Gamma_n$ correspond to decay times introduced to represent the natural radiative relaxation of the level. In this work, every Γ_n will be equal to one small arbitrary Γ_1 value, and f_n and ΔE_n correspond to $2/3(\varepsilon_j^{\vec{k}} - \varepsilon_i^{\vec{k}})\langle \Phi_i^{\vec{k}} | \vec{r} | \Phi_j^{\vec{k}} \rangle \cdot \langle \Phi_j^{\vec{k}} | \vec{r} | \phi_i^{\vec{k}} \rangle$ and $\epsilon_j^{\vec{k}} - \epsilon_i^{\vec{k}}$, respectively, and the summation is over i, j, and $\vec{k}$ with $\Omega(\vec{k})$ weights. The real and imaginary parts of the $\varepsilon(\omega)$ dielectric constant (and conductivity) can then be analytically and separately deduced without performing numerical integration according to the Kramers–Kronig transformation as in Ref. 15. They allow the calculation of the electron-energy loss function (ELF): $-\mathrm{Im}[1/\varepsilon(\omega)]$,[8, 13–15] supposing that the electric dipole approximation still holds ($\hbar\omega < 100\,\mathrm{eV} \Leftrightarrow \lambda > 125\,\text{Å}$).

Computational Details

The calculation of expressions (1) and (2), requires loops on $\vec{k}$-points and occupied $\Phi_i^{\vec{k}}$ and unoccupied $\Phi_j^{\vec{k}}$ orbitals. Owing to the fact that crystalline orbitals are combinations of Bloch functions, $\Sigma_{\vec{g}}\, \chi_\mu^{\vec{g}}(\vec{r}) e^{i\vec{k}\vec{g}}$, which $\chi_\mu^{\vec{g}}(\vec{r})$ is an atomic orbital in the $\vec{g}$-cell of the direct space, itself a combination of Gaussian-type functions, the number of loops becomes important and a parallelization of the program is worth it. This can be done over the external $\vec{k}$-loops because the calculation at each $\vec{k}$-point is independent.

COMPUTATIONAL PARAMETERS FOR BEST (ACCURACY / ELAPSED TIME) RATIO

In both examples (C and Si), convergence of the wave function calculations is reached with 29 $\vec{k}$-points in the reciprocal space. The $\vec{k}$-points generated in CRYSTAL are such that: $\alpha_{xx} \neq \alpha_{yy} \neq \alpha_{zz}$ after having done the weighted sum, which is inconsistent with cubic geometry. This is the result of the $\vec{k}$-points picked out of the irreducible part of the Brillouin zone (IBZ), For example, (100), (010), and (001) equivalent $\vec{k}$-points for which $\alpha_{xx}(100) = \alpha_{yy}(010) = \alpha_{zz}(001)$ in cubic systems are represented by the sole (100) point with a geometrical $\Omega(\vec{k})$ weight and such that $\alpha_{xx}(100) \neq \alpha_{yy}(100) \neq \alpha_{zz}(100) \neq \alpha_{xx}(100)$. Then, to keep this limited number of $\vec{k}$-points (29), only the mean value of the obtained polarizability components, $(\alpha_{xx} + \alpha_{yy} + \alpha_{zz})/3$, is to be considered.

The polarizability calculations converge when the number of dipole moment integrals between two orbitals for which one belongs to the origin cell is such that the other orbital covers only 55 cells in the direct space, that is, the origin cell plus four shells of neighbors (1 + 12 + 6 + 24 + 12) in the cubic-face-centered (CFC) structure. In Table I, we show the central processor unit (CPU) and system times for one $\vec{k}$-point and various numbers of cells. In particular for silicon with a 8-41G** basis set (see applications), the limitation to 55

TABLE I.
CPU and System Times Obtained on an HP 9000 / 735 for 1 $\vec{k}$-point.[a]

Number of cells	1	55	219
CPU time	00:00:42	00:13.40	00:35:50
System time	00:00:00	00:00:00	00:00:08
Total time	00:00:42	00:13:40	00:35.58

[a] Total CPU time is to be multiplied by the Number of $\vec{k}$-points.

cells already leads to a significant time span (13–14 min) as it will be multiplied by the number of $\vec{k}$-points for a complete calculation. It is of interest to compare this time frame to that spent in the CRYSTAL program for Si with 29 $\vec{k}$-points—00:06:20 and 00:16:05 at the HF and LDA levels of calculation, respectively.

PARALLELIZATION TECHNIQUE USED AND RESULTS

The parallel virtual machine (PVM) tool is used because its implementation can be done either in the heterogeneous environment (3 HP 9000/735 and 2 IBM RS 6000/590) or in a homogeneous machine (IBM SP2) at the Centre National Universitaire Sud de Calcul (CNUSC, Montpellier, France).

In Figure 1, CPU times obtained for several numbers of processors are given with computers of various kinds. We note that the CPU time is practically divided by the number of processors used whatever the environment chosen because of the large granularity in parallelization. Thus, the internal loops could be parallelized, but with the use of many more processors. The algorithm could be also improved by optimizing the input–output (I/O).

Applications

The basis sets are those of Orlando et al.[16] (6-21G*) for C and Pisani et al.[17] (8-41G**) for Si. However, in this work, the experimental lattice parameters are chosen as $a = 3.560$ Å and 5.431 Å for the C and Si cubic systems, respectively. Then, each outer *sp* exponent is reoptimized to improve the HF bulk energy. In fact, these new parameters lead to similar polarizability values, with the variation obtained on the static polarizability being less than 1%. Nevertheless, in what follows, the C and Si systems are also studied with the last *d*-type orbital withdrawn from the previous basic sets; that is, with 6-21G and 8-41G* basis sets for C and Si, respectively.

STATIC POLARIZABILITIES

Static polarizabilities and dielectric constants obtained for C and Si with the HF and LDA methods are indicated in Table II, and in Figure 2a and b the electronic band structures along the L–Γ–X–L path (for the richest basis sets) are illustrated. The direct gaps corresponding to the smallest differences, $\varepsilon_j^{\vec{k}} - \varepsilon_i^{\vec{k}}$, obtained at Γ an occur-

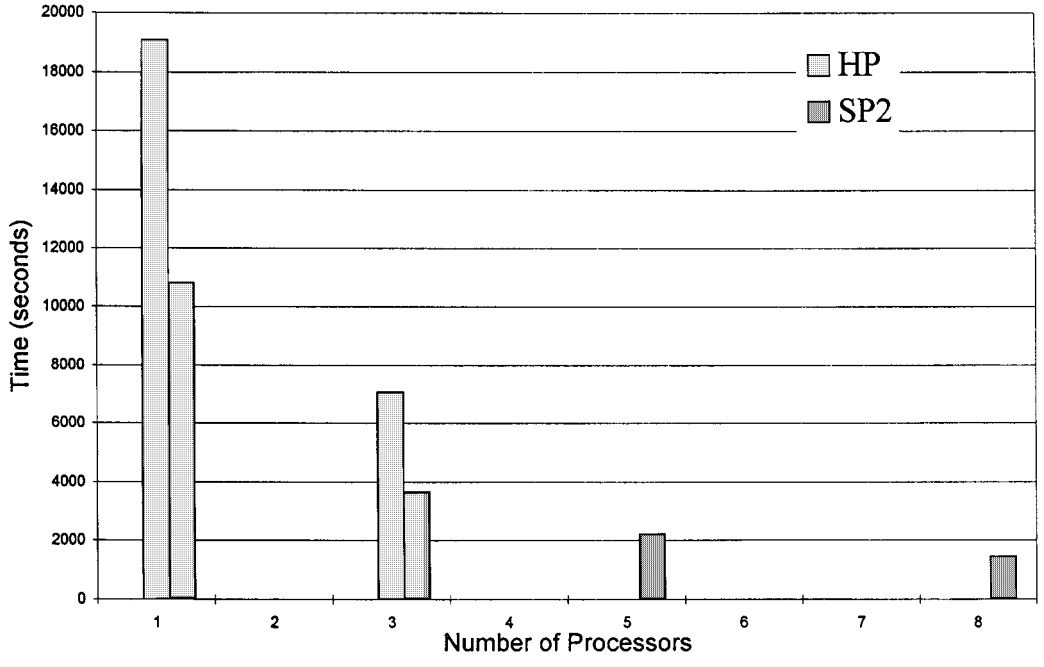

FIGURE 1. CPU times spent for Si (8–41G**, 29 $\vec{k}$-points, 55 cells).

ring in the polarizability calculation, are systematically overestimated by a factor 2 or more with the HF method as presented by Orlando et al.[16] whereas they are underestimated with the LDA method as generally expected for semiconductors[15] by a factor less than 2. The sum over the oscillator strengths, $\sum_n f_n = 2/3\sum_k \Omega(\vec{k})\sum_{i,j}\langle i|\vec{r}|j\rangle_{\vec{k}} \cdot \langle j|\vec{r}|i\rangle_{\vec{k}}(\varepsilon_j^{\vec{k}} - \varepsilon_i^{\vec{k}})$, which should be equal to the number of electrons per cell, is generally too small (except at the HF level for C), especially with the LDA method. This is probably why static atomic polarizability values calculated with the LDA method are close to other calculated and experimental ones: in the sum over states formula, the numerator, as well as the denominator related to the gap is small, and the errors are balanced. It is also of interest to notice that if the conduction band obtained in the HF scheme is shifted by a finite amount to obtain the experimental energy gap, our polarizability HF results are much improved: $\alpha_c = 0.69$ Å^3 and $\alpha_{Si} = 2.86$ Å^3, instead of 0.52 Å^3 and 1.86 Å^3, respectively, without gap correction. This scissors operator method has often been used and gives quite good results even for nonlinear optical parameters.[7] However, our corrected HF polarizability values are still too small, probably because the bandwidths are overestimated, as noted by Orlando et al.[16]

Concerning the last *d*-type orbital, its influence on the polarizability is weak in both cases: 1–2% for C and 3% for Si, showing that the noteworthy effects are not due to our basis sets but rather to the method used (HF or LDA).

In short, in both applications, the uncoupled perturbed LDA method leads to relatively good static polarizability values.

DYNAMIC DIELECTRIC CONSTANTS

To calculate optical properties in solids that can also be obtained from reflectance measurements, the electric field frequency has to be taken into account. Therefore, using eq. (3), we report in Figure 3 the dynamic $\alpha(\omega)$ curves obtained for C and Si until the first resonance corresponding to the direct gap, at the HF and LDA levels, and with the richest basis sets. The corresponding variations of the real and imaginary parts of the dielectric constants are plotted in Figure 4a and b at the LDA level only, in the range $\omega = 0$–1 a.u. and with $\Gamma_1 = 0.005$ a.u. (this latter value leads to arbitrary peak widths qualitatively comparable to those obtained for other cubic systems in Ref. 7). Finally, the behavior of the electron-loss function (ELF) as a function of ω is given in Figure 5a and b at both levels of calculation.

For each system, $\alpha(\omega)$ increases more rapidly with the LDA calculations because of the smaller gap obtained in this approximation. Then, the first total reflections and the first nonzero imaginary parts of the dielectric constants appear at smaller electric field frequencies, comparatively to HF results. In the same way, the ELFs and then the plasma frequencies, indicated by the prominent peaks (Fig. 5a and b), are shifted toward low frequencies with the LDA method. One can also

TABLE II.
Electronic Properties Calculated at the HF and LDA Levels for C and Si in Their Cubic Phase.

	C					Si				
	6–21G		6–21G*			8–41G*		8–41G**		
	HF	LDA	HF	LDA	Other values[a]	HF	LDA	HF	LDA	Other values[a]
Direct gap (eV)	13.17	5.26	13.87	5.33	7.3 [21]	7.69	2.43	8.75	2.72	3.4 [21]
Indirect gap (eV)	11.92	4.09	12.17	3.97	5.4 [9] 5.5 [23]	5.66	0.57	6.32	0.68	1.11 [9]
$\sum_n f_n$ (per atom)	6.01	3.95	6.57	4.49	6	9.71	6.67	10.11	6.9	14
Polarizability (Å^3) per atom	0.53	0.83	0.52	0.83	0.81 [9] 0.82 [9, 22]	1.92	3.50	1.86	3.40	3.71 [10] 3.74 [9] 3.76 [8, 22]
Dielectric Constant	2.95	5.83	2.89	5.98	5.5 [9] 5.7 [8, 22]	3.01	9.09	2.91	8.37	11.4 [10] 11.8 [9] 12.0 [8, 22]

[a] Reference numbers given in brackets.

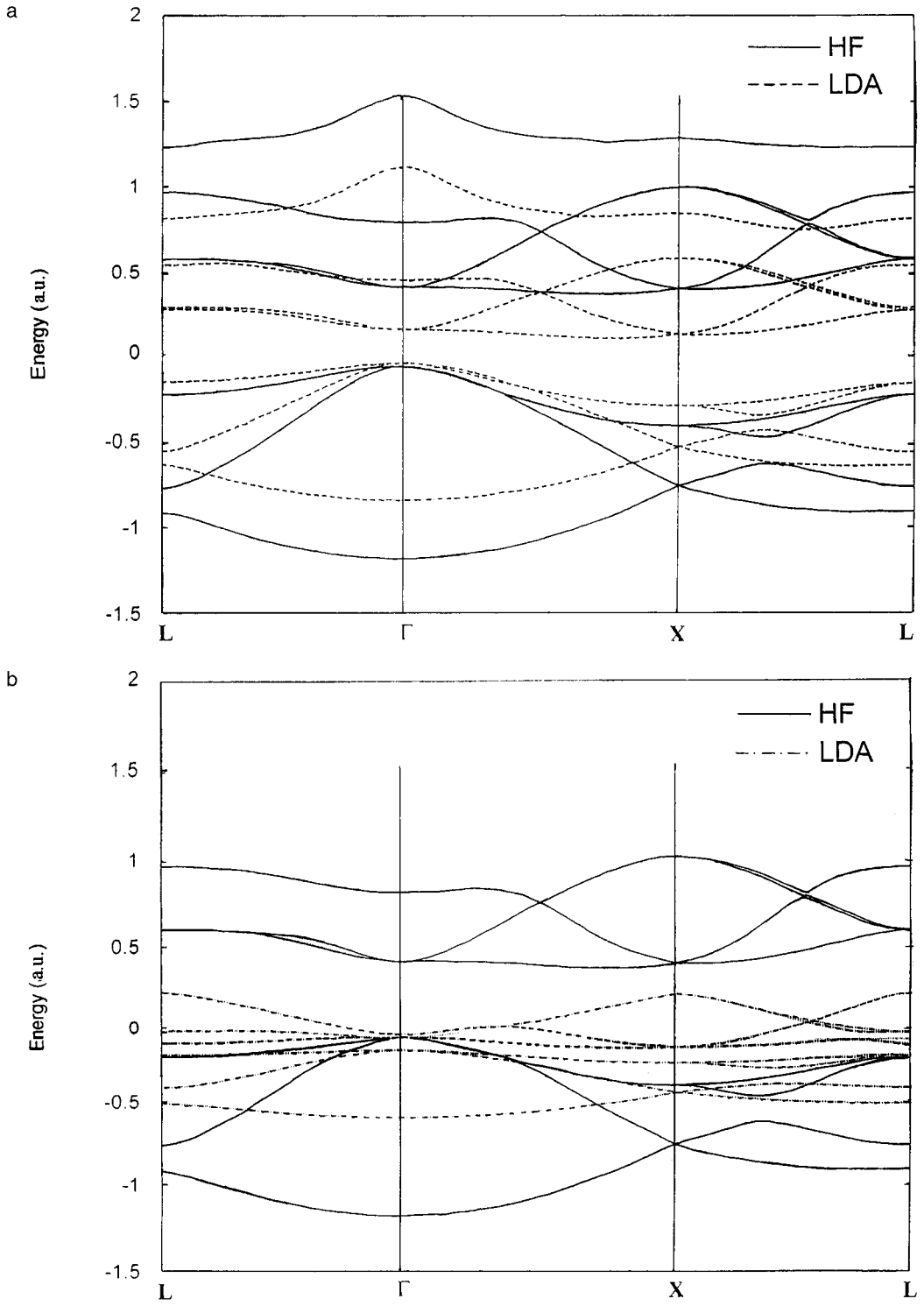

FIGURE 2. (a) Valence and conduction bands of diamond obtained with the 6−21G* basis set. (b) Valence and conduction bands of silicon obtained with the 8−41G** basis set.

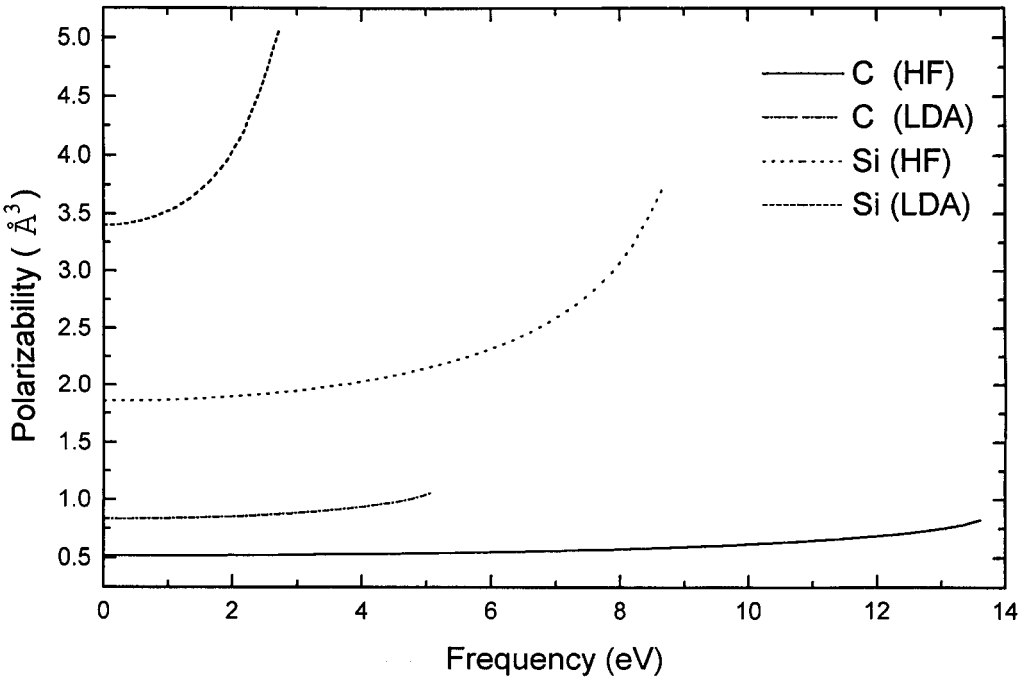

FIGURE 3. Variation of dynamic polarizabilities versus frequency for C and Si at the HF and LDA levels of calculation.

notice the similar shapes obtained at both levels of calculation, but with the smaller energy width for LDA due to more narrow valence and conduction bands (see Fig. 2a and b).

Arguing at the LDA level of calculation for example, valence and conduction widths and diamond gaps are larger than those of silicon. It follows that the static polarizability is smaller for C than for Si all the more because the sum of oscillator strengths (or α-numerator) should be equal to 6 for C and 14 for Si, and that the ELF of diamond was spread out much more than that of silicon.

Conclusion

In this work, we have investigated an uncoupled perturbation program (UCLDA) allowing for simple calculation of dynamic polarizabilities, dielectric constants, and electron loss energy functions of periodic systems after having obtained crystal orbitals via a periodic self-consistent field process implemented in the CRYSTAL program at both the HF and LDA levels. Moreover, the parallelized version of the (UCLDA) program was shown to lead to rapid estimations of the optical properties.

For both C and Si cubic systems, the LDA results, for which correlation effects are taken into account, are better than the HF results and are even in good agreement with experimental values despite the approximation made. In fact, oscillator strengths obtained from LDA wave functions were found to be weak, but the error in the numerators of α is balanced by a small gap. In contrast, HF oscillator strength values were shown to be relatively good, but the gap was too large. In this latter case, a scissors operator is necessary. Another method could be the use of a perturbation theory of electron correlation effects, similar to the study of infinite polyenes by Suhai.[18]

Finally, the study of these similar C and Si crystals allows to confirm the more conductor character of silicon compared to that of diamond.

Acknowledgment

Financial support from the Human Capital Mobility Program of the European Union under Contract No. CHRX-CT91-0155 is gratefully acknowledged. We also thank the Institut du Développement et des Ressources en Informatique et Scientifique (IDRIS) of the Centre National Uni-

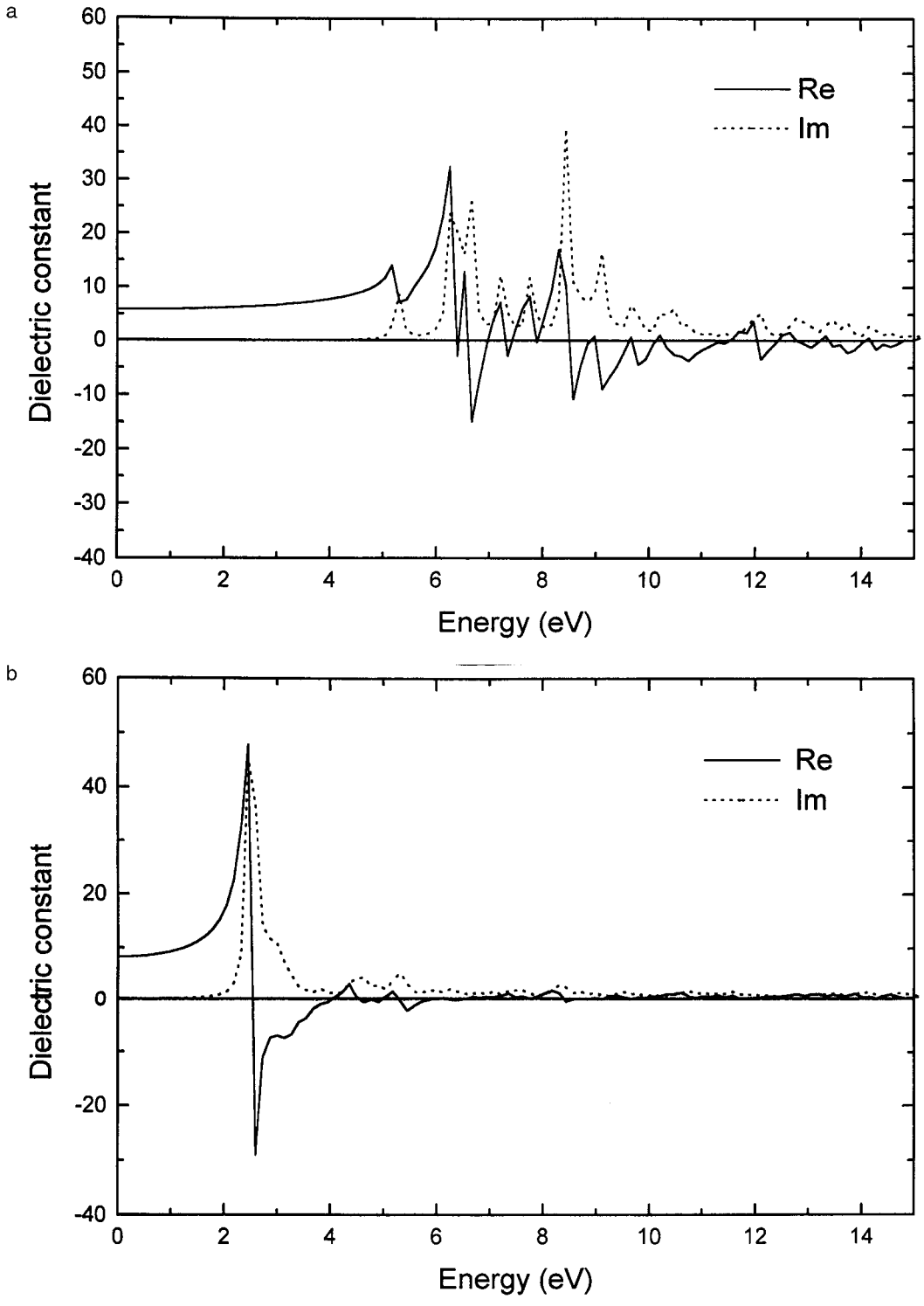

FIGURE 4. (a) Plots of calculated real and imaginary parts of the dielectric constant of diamond with the 6−21G* basis set at the LDA level of calculation. (b) Plots of the calculated real and imaginary parts of the dielectric constant of silicon with the 8−41G** basis set at the LDA level of calculation.

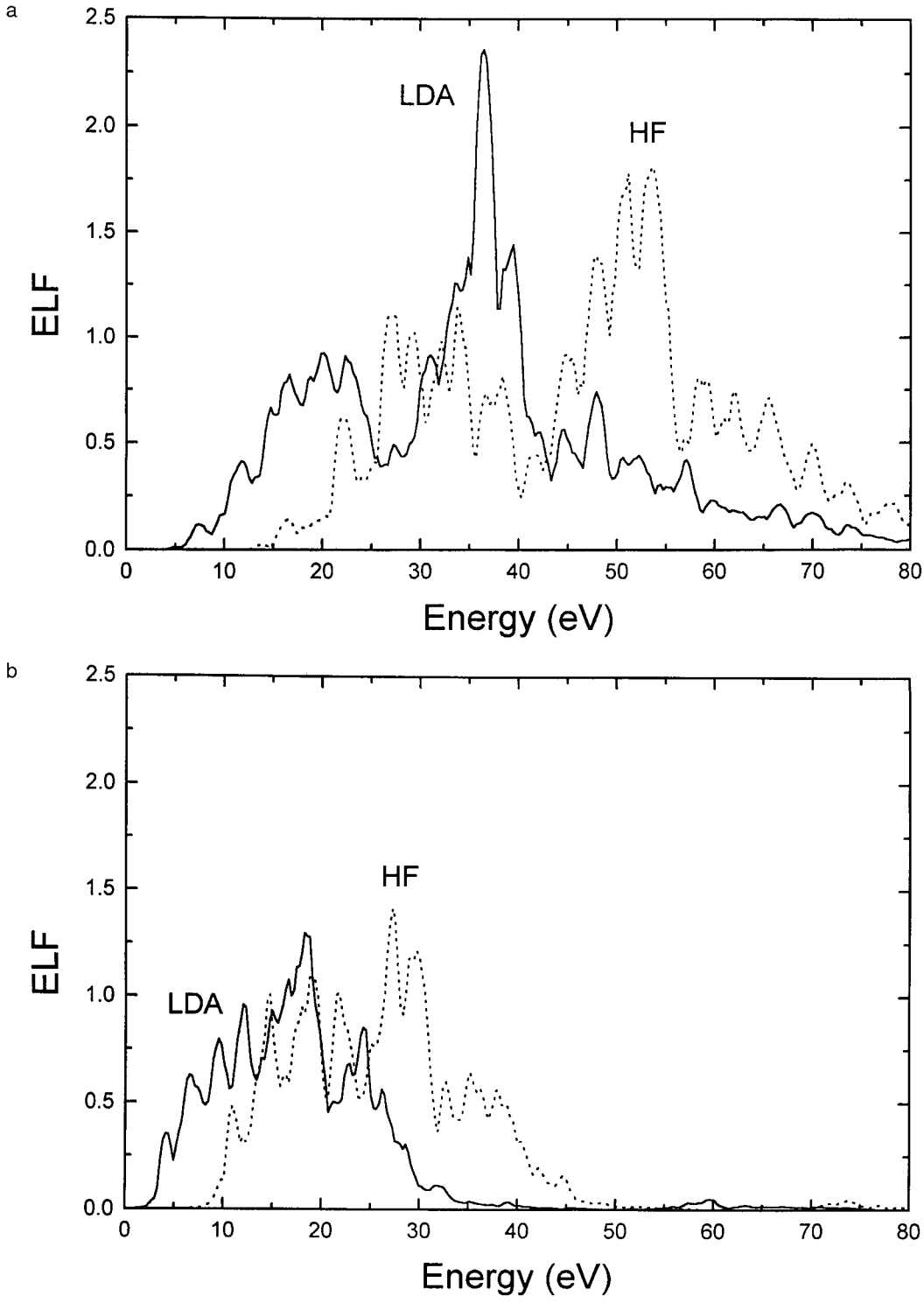

FIGURE 5. (a) Electron loss function of diamond obtained with the 6−21G* basis set at both levels of calculation. (b) Electron loss function of silicon obtained with the 8−41G** basis set at both levels of calculation.

versitaire Sud de Calcul (CNUSC) for their support.

Appendix: Calculation of Dipole Moment Transitions

Crystalline $\Phi_l^{\vec{k}}$ orbitals are developed on the Bloch $\varphi_\mu^{\vec{k}}$ functions:

$$\Phi_l^{\vec{k}} = \sum_\mu C_{i\mu}^{\vec{k}} \varphi_\mu^{\vec{k}} \qquad \text{with}$$

$$\varphi_\mu^{\vec{k}} = \frac{1}{\sqrt{N}} \sum_{\vec{g}} \chi_\mu(\vec{g}) e^{i\vec{k}\cdot\vec{g}}$$

with N being the number of $\vec{g}$-cells and $\chi_\mu(\vec{g})$ an atomic orbital in the $\vec{g}$-cell. Then, dipole transition integral between crystalline orbitals are equal to:

$$\langle \Phi_i^{\vec{k}} | \vec{r} | \Phi_j^{\vec{k}'} \rangle = \sum_{\mu,\nu} C_{i\mu}^{*\vec{k}} C_{j\nu}^{\vec{k}'} \langle \varphi_\mu^{\vec{k}} | \vec{r} | \varphi_\nu^{\vec{k}'} \rangle$$

Let us calculate the following integral:

$$I = \left\langle \varphi_\mu^{\vec{k}} | \vec{r} | \varphi_\nu^{\vec{k}'} \right\rangle = \frac{1}{N} \sum_{\vec{g},\vec{g}'} \left\langle \chi_\mu(\vec{g}) | \vec{r} | \chi_\nu(\vec{g}') \right\rangle e^{i(\vec{k}'\cdot\vec{g}' - \vec{k}\cdot\vec{g})}$$

With the dipole moment $\langle \chi_\mu(\vec{g}) | \vec{r} | \chi_\nu(\vec{g}') \rangle$ transition being split in:

$$\left\langle \chi_\mu(\vec{g}) | \vec{r} - \vec{g} | \chi_\nu(\vec{g}') \right\rangle + \vec{g} \left\langle \chi_\mu(\vec{g}) | \chi_\nu(\vec{g}') \right\rangle$$

we can write:

$$I = \frac{1}{N} \sum_{\vec{g},\vec{g}'} \left[\langle \chi_\mu(\vec{g}) | \vec{r} - \vec{g} | \chi_\nu(\vec{g}') \rangle + \vec{g} \langle \chi_\mu(\vec{g}) | \chi_\nu(\vec{g}') \rangle \right] e^{i(\vec{k}'-\vec{k})\cdot\vec{g}} e^{i\vec{k}'\cdot(\vec{g}'-\vec{g})}$$

$$= \frac{1}{N} \sum_{\vec{g},\vec{g}''} \left[\langle \chi_\mu(\vec{0}) | \vec{r} | \chi_\nu(\vec{g}'') \rangle + \vec{g} \langle \chi_\mu(\vec{0}) | \chi_\nu(\vec{g}'') \rangle \right] e^{i(\vec{k}'-\vec{k})\cdot\vec{g}} e^{i\vec{k}'\cdot\vec{g}''}$$

with $\vec{g}'' = \vec{g}' - \vec{g}$ and after changing the $\vec{r}$ variable into $\vec{r} + \vec{g}$ in the integrals. With $\vec{g}$ and $\vec{g}''$ being independent and running over the cells of the infinite crystal, we have:

$$I = \frac{1}{N} \sum_{\vec{g}} e^{i(\vec{k}'-\vec{k})\vec{g}} \left[\sum_{\vec{g}''} \langle \chi_\mu(\vec{0}) | \vec{r} | \chi_\nu(\vec{g}'') \rangle e^{i\vec{k}'\cdot\vec{g}''} + \vec{g} \sum_{\vec{g}''} \langle \chi_\mu(\vec{0}) | \chi_\nu(\vec{g}'') \rangle e^{i\vec{k}'\cdot\vec{g}''} \right]$$

$$= \frac{A}{N} \sum_{\vec{g}} e^{i(\vec{k}'-\vec{k})\vec{g}} + \frac{B}{N} \sum_{\vec{g}} \vec{g} e^{i(\vec{k}'-k)\vec{g}}$$

where $A = \Sigma_{\vec{g}''} \langle \chi_\mu(\vec{0}) | \vec{r} | \chi_\nu(\vec{g}'') \rangle e^{i\vec{k}'\cdot\vec{g}''}$ and $B = \Sigma_{\vec{g}''} \langle \chi_\mu(\vec{0}) | \chi_\nu(\vec{g}'') \rangle e^{i\vec{k}'\cdot\vec{g}''}$. With $\vec{k}' - \vec{k}$ being a vector of the Brillouin zone, we have:

$$\sum_{\vec{g}} e^{i(\vec{k}'-\vec{k})\vec{g}} = N\delta_{\vec{k},\vec{k}'}$$

because of the Born–Von Karman hypothesis used in the CRYSTAL program.

Then, for $\vec{k} = \vec{k}'$, the expression of I becomes:

$$I = \sum_{\vec{g}} \left\langle \chi_\mu(\vec{0}) | \vec{r} | \chi_\nu(\vec{g}) \right\rangle e^{i\vec{k}\cdot\vec{g}}$$

with the second term being null because we have $\Sigma_{\vec{g}} \vec{g} = \vec{0}$ in our calculations.

When $\vec{k} \neq \vec{k}'$, the first term of I is then equal to zero, but it is not obvious to neglect the second one. However:

- $1/N \, \Sigma_{\vec{g}} \vec{g} e^{i(\vec{k}'-\vec{k})\cdot\vec{g}}$, which is not longer equal to zero, tends to zero for very different $\vec{k}$- and $\vec{k}'$-points; effectively in the one-dimension case to simplify:

$$\lim_{L\to\infty} \frac{a_0}{2L+1} \sum_{l=-L}^{+L} 1 e^{il(2\pi/2L+1)p} = \pm \frac{ia_0}{\pi p}$$

with p being a nonzero integer belonging to $[-L, +L]$ and such that:

$$k - k' = \frac{p}{a_0} \times \frac{2\pi}{2L+1}$$

and a_0 a lattice parameter (this result is obtained by replacing the discrete sum with an integration). If L is a large number, $\vec{k}$ and $\vec{k}'$ differ for large p-values, so that the previous sum is small.

- B terms are overlaps between $\varphi_\mu^{\vec{k}'}$ and $\varphi_\nu^{\vec{k}'}$ Block functions with the same $\vec{k}'$-point. They are not equal to zero, but, in contrast to the precedent case, their contribution to the dipole transition from the occupied $\Phi_i^{\vec{k}}$ to

the unoccupied $\Phi_j^{\vec{k}'}$ orthogonal crystalline orbitals after the summation over $C_{i\mu}^{*\vec{k}} C_{j\nu}^{\vec{k}'}$ is probably weak when $\vec{k}$ and $\vec{k}'$ are very closed: $C_{i\mu}^{*\vec{k}'} \approx C_{i\mu}^{*\vec{k}} \Rightarrow \langle \Phi_i^{\vec{k}} \mid \Phi_j^{\vec{k}'} \rangle \approx \langle \Phi_i^{\vec{k}} \mid \Phi_j^{\vec{k}} \rangle = 0 \; (i \neq j)$.

The second term of I can then be dropped and only the vertical transitions ($\vec{k} = \vec{k}'$) are taken into account in our calculation (see also Ref. 19):

$$\left\langle \Phi_i^{\vec{k}} | \, \vec{r} \, | \Phi_j^{\vec{k}} \right\rangle = \sum_{\mu,\,\nu} C_{i\mu}^{*\vec{k}} C_{i\nu}^{\vec{k}} \sum_{\vec{g}} \left\langle \chi_\mu(\vec{0}) \mid \vec{r} \mid \chi_\nu(\vec{g}) \right\rangle e^{i\vec{k}\cdot\vec{g}}$$

These moment integrals are finite, as shown by Ladik,[20] because $\chi_\mu(\vec{0})$ and $\chi_\nu(\vec{g})$ are combinations of Gaussian functions tending to zero much more quickly than $\vec{r}$ tends to infinity.

References

1. R. Dovesi, V. R. Saunders, and C. Roetti, CRYSTAL92 User Documentation, University of Torino (Italy) and SERC Daresbury Laboratory (UK).
2. A. Lichanot and M. Rérat, *Chem. Phys. Lett*. **211**, 249 (1993).
3. P. Azavant, A. Lichanot, M. Rérat, and C. Pisani, *Acta Cryst. B* **50**, 279 (1994).
4. A. Lichanot, M. Rérat, and M. Causá, *J. Phys. Condens. Matter*, **8**, 10425 (1996).
5. *M. Causá and A. Zupan*, *Int. J. Quant. Chem. Quant. Chem. Symp*. **28**, 633 (1994).
6. B. Champagne, J. G. Fripiat, and J. M. André, *J. Chem. Phys*., **96**, 8330 (1992).
7. W. Y. Ching, F. Gan, and M. Z. Huang, *Phys. Rev. B*, **52**, 1596 (1995).
8. N. W. Ashcroft and N. D. Mermin, In *Solid State Physics*, Holt, Rinehart and Winston, New York, 1976.
9. *CRC Handbook and Chemistry and Physics*, *69th Edition*, CRC Press, Boca Raton, FL, 1988–1989.
10. A. Dal Corso, S. Baroni, and R. Resta, *Phys. Rev. B*, **49**, 5323 (1994).
11. J. P. Perdew and A. Zunger, *Phys. Rev. B*, **23**, 5048 (1981).
12. D. M. Ceperley and B. J. Alder, *Phys. Rev. Lett*., **45**, 566 (1980).
13. J. M. Ziman, In *Principles of the Theory of Solids*, Cambridge University Press, Cambridge, UK, 1969.
14. C. Kittel, In *Physique de l'état Solide*, *Dunod Université Édition*, Wiley, New York, 1976.
15. S. D. Mo and W. Y. Ching, *Phys. Rev. B*, **51**, 13023 (1995).
16. R. Orlando, R. Dovesi, C. Roetti, and V. R. Saunders, *J. Phys. Condens. Matter*, **2**, 7769 (1990).
17. C. Pisani, R. Dovesi, and R. Orlando, *Int. J. Quant. Chem*., **42**, 5 (1992).
18. S. Suhai, *Int. J. Quant. Chem*., **42**, 193 (1992).
19. B. Champagne and J. M. André, *Int. J. Quant. Chem*., **42**, 1009 (1992).
20. J. Ladik, *J. Mol. Struct*., **206**, 39 (1990).
21. R. W. Godby, M. Schulter, and L. J. Sham, *Phys. Rev. B*, **36**, 6497 (1987).
22. J. C. Phillips, *Phys. Rev. Lett*., **20**, 550 (1968).
23. F. J. Himpsel, J. F. Van der Veen, and D. E. Eastman, *Phys. Rev. B* **22**, 1967 (1980).